2026 IEEE/SICE International Symposium on System Integration (SII)
January 11-14, 2026. Cancún, México

Quantitative Evaluation of Energy Savings in a 3-DOF Manipulator via Lightweighting with Plastic Structural Parts

Kenji Sekiguchi[1], Norisato Kanai[1], Yuta Tsukamoto[1], Hiroyuki Nabae[1], Takahiro Aruga[1], Takeshi Takaki[2], Naoyuki Takesue[3], Yusuke Ota[4], Gen Endo[1]

Abstract— **This research quantitatively evaluates the energy-saving effects of lightweighting the structural parts of industiral robots by substituting conventional aluminum alloys with plastics. We prototyped three types of 3-DOF vertically articulated robots with structural parts made of A5052 aluminum alloy, a carbon fiber non-woven composite (Feltcarbon), and a 3D-printed composite (Onyx+CF). We then measured the energy consumption of each joint and the total manipulator during a 10-cycle pick-and-place task. The results show that replacing the aluminum alloy with Feltcarbon and Onyx+CF reduces the manipulator's total energy consumption by 25% and 30%, respectively. At the single-joint level, maximum energy savings reached 44% for Feltcarbon and 53% for Onyx+CF compared to the A5052 baseline.**

I. INTRODUCTION

Industrial robots, characterized by their high positioning accuracy and operational repeatability, are widely used in manufacturing to enhance productivity and quality. In recent years, reducing their energy consumption has become a key priority, motivated by the need to minimize both environmental impact and operating costs. The energy consumption of industrial robots is significant, representing approximately 8% of total energy consumption in manufacturing[1]. Furthermore, with energy-related costs constituting approximately 60% of a robot's total operating costs[2], enhancing their efficiency is not merely an ecological consideration but a crucial economic priority.

To reduce the energy consumption of industrial robots, numerous methods have been considered from both hardware and software perspectives. Hardware-based approaches focus on weight reduction, including combining Carbon Fiber Reinforced Plastics (CFRP) with aluminum alloy (A5052) for structural parts[3], and utilizing topology optimization[4]. In contrast, software-based methods include optimizing robot motion parameters[5], energy-efficient motion planning using dynamic scaling[6], and path planning that avoids excessive acceleration and incorporates low-torque waiting postures[7]. However, the effectiveness of software-based methods is often limited to specific tasks and may not guarantee consistent results. Furthermore, optimizing complex trajectories is computationally intensive and can increase task time compared to Point-to-Point (PTP) movements. In contrast, hardware-based weight reduction directly decreases the joint torques acting on a robot, offering a more straightforward path to lower power consumption. This effect is particularly significant for vertically articulated robots in a horizontal posture, where joint torque increases proportionally with link mass. Therefore, combining lightweight design with trajectory optimization methods is expected to yield even greater reductions in energy consumption.

Therefore, our research group focuses on reducing weight by substituting plastics for the conventional metals used in the structural parts of industrial robots. The design of these parts requires an evaluation of the following two characteristics, in addition to the standard evaluation of strength and stiffness.

The first characteristic is damping performance. Weight reduction enables industrial robots to operate at higher speeds, improving productivity by shortening task times. However, to reduce task times, vibrations at the end-effector must be rapidly damped upon reaching its target position. This necessitates structural materials with excellent vibration-damping properties. In a previous study, we evaluated this characteristic using a one-degree-of-freedom (1-DOF) experimental apparatus consisting of an actuator with a harmonic drive and a simplified link specimen[8]. A comparison of seven types of plastic materials and four types of aluminum alloys confirmed that while the damping ratios of the plastics were comparable to those of the aluminum alloys, their lower stiffness led to larger vibration amplitudes and, consequently, longer settling times. In that evaluation, we found that a carbon fiber non-woven composite (Feltcarbon, Futaba)[9] exhibited a small amplitude while maintaining a high damping ratio, resulting in a short settling time. Furthermore, it was found that reinforcing 3D-printed plastics with continuous carbon fibers achieved a similar desirable outcome, shortening the settling time.

The second characteristic is creep performance. Creep is the tendency of a material to deform gradually over time when subjected to a constant external force. At room temperature, metal materials generally do not exhibit creep, but plastic materials do. For industrial robots intended for long-term continuous use, this characteristic can alter the relative positions of the joints, leading to a reduction in the end-effector's positioning accuracy and repeatability. We hypothesize that by understanding the trends and amount of creep deformation in plastics, we can calibrate the ma-

[1]Department of Mechanical Engineering, School of Engineering, Institute of Science Tokyo, 2-12-1 Ookayama, Meguro-ku, Tokyo 152-8550, Japan, tsukamoto.y.ak@m.titech.ac.jp.
[2]The Smart Robotics Lab, Graduate School of Advanced Science and Engineering, Hiroshima University, Hiroshima, Japan.
[3]Department of Mechanical Systems Engineering, Graduate School of Systems Design, Tokyo Metropolitan University, Japan.
[4]Department of the Advanced Robotics, Chiba Institute of Technology, 2-17-1 Tsudanuma, Narashino, Chiba 257-0016, Japan.

978-1-6654-5784-2/26/$31.00 ©2026 IEEE

nipulator's control to compensate for the positional error. Therefore, we measured creep deformation over approximately two months for six types of specimens: five plastics and the aluminum alloy (A5052)[10]. The experiment used a cantilever beam setup where one end of a specimen was fixed and a concentrated load was applied to the other. The results revealed that Feltcarbon, much like A5052, exhibited minimal deformation, with almost no creep occurring. For the 3D-printed plastics, it was found that reinforcement with continuous carbon fibers could effectively suppress creep deformation. Additionally, we measured creep deformation of 3D printed plastic specimens with different matrix infill ratios and varied orientations of long carbon fibers[11]. The results revealed that orienting long carbon fibers perpendicular to the load direction effectively suppresses creep deformation.

As shown above, we have confirmed improvements in the damping and creep characteristics of specific plastic materials, indicating their applicability for structural parts of industrial robots. Building on these findings, this study quantitatively evaluates the reduction in power consumption achieved by such lightweighting. However, we cosider that the simulation-based evaluation of power consumption for a plastic-based lightweight industrial robot is difficult. As for this problem, the following three issues are considered.

1) There is no established design methodology for industrial robot parts made of plastic materials. It is therefore necessary to develop this methodology by actually designing, manufacturing, and evaluating parts made with the corresponding plastic materials. Based on this process, appropriate metrics must be established to guide the substitution of metal components with plastic ones. Consequently, as long as these crucial metrics are missing, it is impossible to build a valid model of the industrial robot, preventing us from obtaining any useful simulation results.
2) Servomotors, commonly used as actuators in industrial robots, deliver their output through a gear reducer. However, it is difficult to accurately model this reducer, including factors like the effects of the gear ratio and friction within the internal gears. This challenge, in turn, makes it hard to obtain useful simulation results.
3) Servomotors in industrial robots operate in conjunction with servo amplifiers. These amplifiers can have a significant standby energy consumption. If this standby power is high while the motor's own consumption from torque is low, the energy-saving effects of making the robot lighter may be completely negated. Furthermore, if the amplifier is equipped with features like energy recovery through regeneration, the effects of lightweighting might also be unobserved during the manipulator's dynamic acceleration and deceleration. Therefore, to accurately assess any power reduction from lightweighting, it's essential to first determine the overall impact of the servo amplifier. We consider that a proper evaluation is impossible without running a simulation that explicitly accounts for the amplifier's influence on total power consumption.

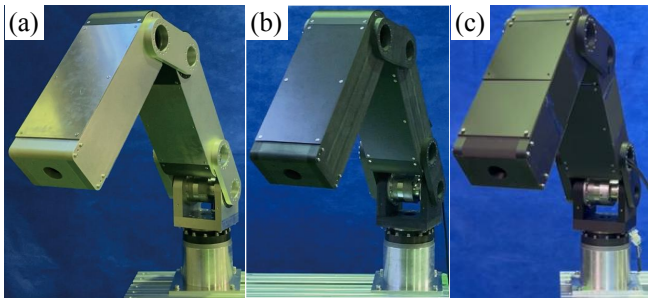

Fig. 1. 3-DOF manipulator: (a) Made of A5052, (b) Made of Feltcarbon, (c) Made of 3D printed parts.

Therefore, as a foundational evaluation for resolving these issues, this study aims to quantitatively evaluate the reduction in energy consumption achieved by lightweighting industrial robots. We fabricated a manipulator in which the traditionally used aluminum alloy structural parts have been replaced with plastic materials. We then assessed the energy savings by measuring the power consumption of modified manipulators. We focused on two materials: Feltcarbon and a 3D-printed plastic reinforced with continuous carbon fibers. Using these two plastics alongside the A5052, we prototyped three versions of a three-degree-of-freedom (3-DOF) manipulator, as shown in Fig. 1. We then evaluated the energy-saving effect of lightweighting these parts by comparing the power consumption of each manipulator as it performed a simulated pick-and-place operation.

II. Design of Manipulator

Fig. 2 shows a schematic of the manipulator, and its specifications are listed in Table I. The manipulator is mounted on a base. For the posture shown in Fig. 2, we established a right-hand coordinate system: the Z-axis is vertically upward, the X-axis is in the direction of the arm's extension, and the Y-axis is perpendicular to both. Rotations around the X, Y, and Z-axes are defined as roll, pitch, and yaw, respectively. In this manipulator, the base joint (Joint 1 (J1)) provides yaw

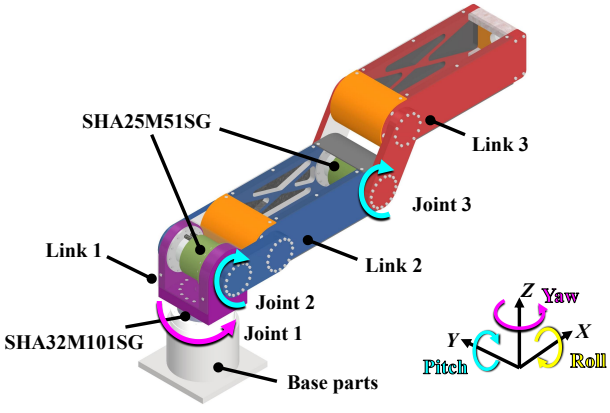

Fig. 2. Schematic diagram of the 3-DOF manipulator.

TABLE I

SPECIFICATIONS OF THE 3-DOF MANIPULATOR.

Specifications	Values
Degree of freedom	3
Motor output	170 W (SHA25M51SG) 370 W (SHA32M101SG)
Motor amplifier	MR-J4-60B-S033 (SHA25M51SG) MR-J4-100B-S033 (SHA32M101SG)
Range of motion for each axis	J1: $\pm$ 180 deg J2: $\pm$ 110 deg J3: $\pm$ 120 deg
Maximum arm length	940 mm

TABLE II

SPECIFICATIONS OF AC SERVO MOTORS.

Specifications	SHA32M101SG	SHA25M51SG
Reduction ratio	1:101	1:51
Maximum continuous torque	178 Nm	41 Nm
Maximum torque	433 Nm	127 Nm

TABLE III

MECHANICAL PROPERTIES[9][12][13][14].

Material	A5052	Feltcarbon	Onyx	CF
Density [g/cm^3]	2.7	1.3	1.2	1.4
Tensile strength [MPa]	268	270	40	800
Tensile modulus [GPa]	68	22	2.4	60
Bending strength [MPa]	-	300	71	540
Bending modulus [GPa]	-	18	3.0	51

TABLE IV

MASS OF EACH PART OF 3-DOF MANIPULATORS.

Each parts	A5052	Feltcarbon	Onyx+CF
SHA32M101SG	6.2 kg	6.2 kg	6.2 kg
SHA25M51SG	3.1 kg $\times$ 2	3.1 kg $\times$ 2	3.1 kg $\times$ 2
Link1 (Purple parts)	2.3 kg	1.2 kg	0.64 kg
Link2 (Blue parts)	6.2 kg	3.3 kg	1.8 kg
Link3 (Red parts)	7.2 kg	3.9 kg	2.1 kg
Base parts	2.7 kg	2.7 kg	2.7 kg
Total	30.8 kg	23.5 kg	19.7 kg

rotation, while the shoulder (Joint 2 (J2)) and elbow (Joint 3 (J3)) joints provide pitch rotation. As shown in Fig. 2, the parts colored purple, blue, and red are designated as Link 1, Link 2, and Link 3, respectively. The joints are actuated by AC servo motors. J1 uses an SHA32M101SG (Harmonic Drive Systems), while J2 and J3 both use an SHA25M51SG (Harmonic Drive Systems). Table II details key specifications for these motors, including their gear reduction ratios, rated continuous torques, and maximum torques. These motors are integrated units that feature a hollow-shaft harmonic gear reducer and deliver output from a flange. Therefore, at each joint, the motor's flange is fastened directly to the corresponding link with screws, transmitting the actuator's torque to the structure.

Fig. 3 shows the dimensions of each link. In this design, the segment of Link 3 with length l_a is attached to Link 2 at a 60 degree angle about the Y-axis. This configuration addresses a potential issue: if segments l_a and l_b of Link 3 were collinear, the orange part of Link 3 (shown in Fig. 2) would collide with the side of Link 2 when J3 rotates more than 123 degrees. This collision would constrain the manipulator's range of motion. Since industrial robots often perform pick-and-place tasks near their base, ensuring the manipulator can operate freely in this workspace is crucial. An offset was implemented between Link 2 and Link 3, and a corresponding offset was created within Link 3 itself between segments l_a and l_b. These offsets prevent mechanical interference and expand the manipulator's overall operational workspace.

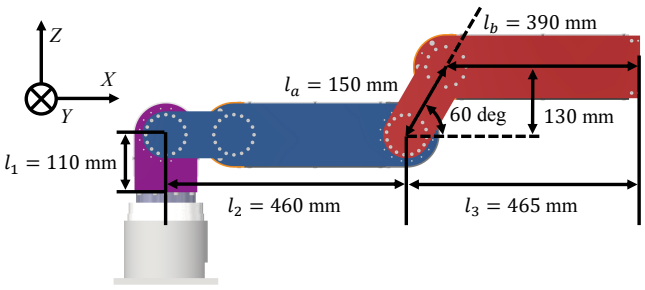

Fig. 3. Length of individual parts of the 3-DOF manipulator.

To evaluate the effects of lightweighting the structural parts, we prototyped three versions of the manipulator using different materials: A5052 aluminum alloy as a comparative baseline, Feltcarbon, and a 3D-printed plastic reinforced with continuous carbon fiber. Feltcarbon is produced by laminating layers of non-woven carbon fiber fabric with a thermosetting plastic, followed by high-pressure molding and machining. As a result, unlike conventional CFRP, it exhibits high machinability and near-isotropic mechanical properties. The 3D-printed components were fabricated on a printer (X7, Markforged) using a short carbon fiber reinforced nylon filament (Onyx, Markforged)[12], and reinforced with a continuous carbon fiber reinforced nylon filament (CF, Markforged)[13]. The printing parameters were a 0.125 mm layer height, 37% infill density with a triangular structure, four top and bottom solid layers, and two walls (shells). Additionally, a reinforcement wall of CF was laid down just inside the outer shells of each part. Table III lists the mechanical properties of these materials, and Table IV shows the mass of each part for the manipulators. Since each manipulator uses the same actuators (SHA32M101SG, SHA25M51SG), the actuator mass is identical across all versions. However, the mass of the link parts alone shows significant differences: 15.7 kg for A5052, 8.4 kg for Feltcarbon, and 4.54 kg for Onyx+CF. Thus, replacing the A5052 with Feltcarbon and Onyx+CF reduces the link mass by 46% and 71%, respectively. For the manipulator as a whole, this material substitution results in total mass reductions of 24% and 36%, respectively.

The selected materials have manufacturing-related size limitations. For Feltcarbon, the maximum available size is 300 mm $\times$ 450 mm for plate thickness between 10 mm and 30 mm, and this reduces to 300 mm $\times$ 300 mm for thicknesses between 30 mm and 45 mm. Similarly, the 3D-printed parts are constrained by the printer's 330 mm $\times$

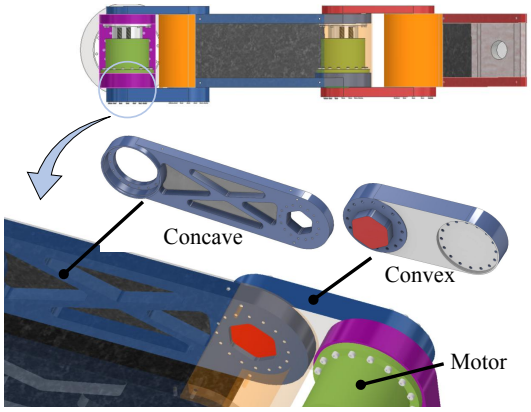

Fig. 4. Fitting the interlocking parts of the 3-DOF manipulator.

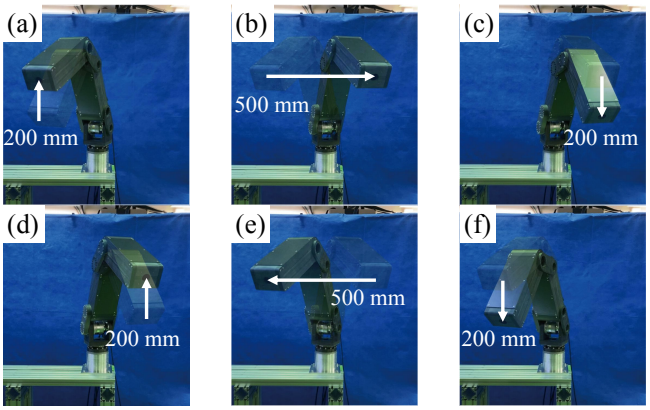

Fig. 5. Target trajectory for evaluating the energy consumption of 3-DOF manipulators.

270 mm × 200 mm build volume. To overcome these size limitations, we adopted a technique previously validated by our research group: using interlocking hexagonal features to effectively transmit torque in low-stiffness materials by reducing surface pressure[15]. Accordingly, for Link 2, we designed parts with these interlocking features, as shown in Fig. 4. By fitting and fastening these multiple parts together with screws, we could fabricate links with dimensions larger than the individual manufacturing constraints. This same method was also used for Link 3. The previously mentioned offset joint, which connects the l_a and l_b segments, was constructed by incorporating these hexagonal features into the separate parts, which were then mated and fastened with screws.

III. Evaluation of Energy Consumption

This section evaluates the reduction in power consumption achieved by lightweighting the manipulator's structural parts. To achieve this, we measured the power consumed by the three manipulator versions (A5052, Feltcarbon, and 3D-printed plastic) as they performed a pick-and-place task. This operation was selected because it represents a fundamental handling task for industrial robots.

A. Conditions for the evaluation

The pick-and-place task followed the motion sequence illustrated in Fig. 5. Starting from an initial position, the manipulator executes an outbound sequence:

(a) A 200 mm upward movement.
(b) A 500 mm horizontal movement.
(c) A 200 mm downward movement.

This is followed by a return sequence to the initial position:

(d) A 200 mm upward movement.
(e) A 500 mm horizontal movement in the reverse direction of step (b).
(f) A 200 mm downward movement.

For this experiment, we define a single cycle as a one-way trip, comprising either the outbound sequence (a-c) or the return sequence (d-f). Power consumption was measured and compared over a total of 10 cycles, equivalent to 5 full round trips.

To measure the manipulator's power consumption, we measured the AC current on Phase 1 of the three-phase, 200 V power line supplying each servo amplifier from the distribution panel. This method was chosen to capture the total power consumed by all components required to drive the manipulator, including the AC servo motors and their amplifiers. The current was measured using a compact data logger (ZN-CTX21 with a ZN-CTS11-5A sensor, OMRON). This current result was then converted to power consumption by multiplying it by the line voltage and an assumed power factor of 0.8. All data was sampled at a frequency of 10 Hz.

B. Result of the measurement

Fig. 6, Fig. 7, and Fig. 8 show the results for joints J1, J2, and J3, respectively. In these figures, the lines represent the average power consumption per cycle for each joint: green for the A5052 manipulator, red for the Feltcarbon manipulator, and blue for the 3D-printed manipulator.

First, for Joint 1, the peak power consumption was 144 W for the A5052, 133 W for Feltcarbon, and 129 W for the 3D-printed version. This corresponds to relatively small power reductions of 7.6% and 10.6% when replacing A5052 with

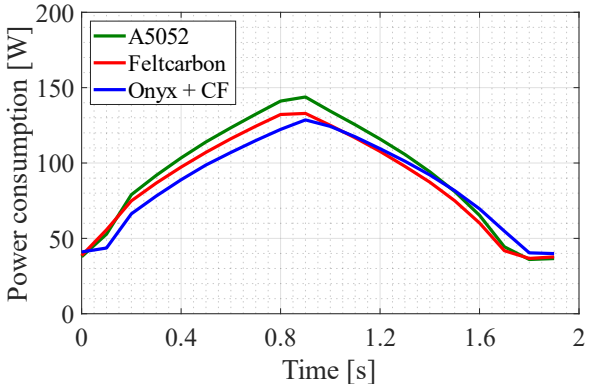

Fig. 6. Comparison of power consumption at J1: (Green line) A5052, (Red line) Feltcarbon, (Blue line) Onyx + CF.

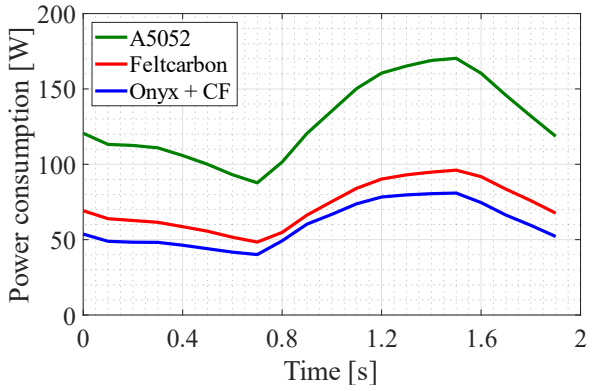

Fig. 7. Comparison of power consumption at J2: (Green line) A5052, (Red line) Feltcarbon, (Blue line) Onyx + CF.

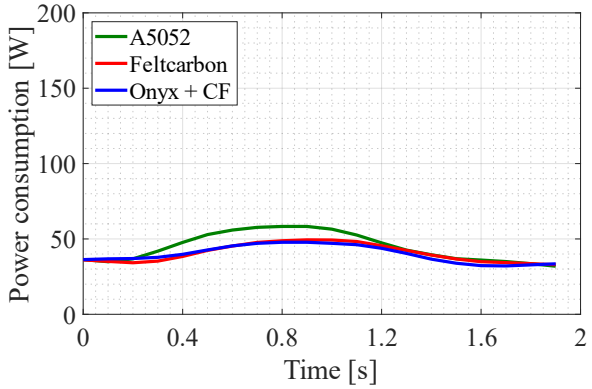

Fig. 8. Comparison of power consumption at J3: (Green line) A5052, (Red line) Feltcarbon, (Blue line) Onyx + CF.

Feltcarbon and 3D-printed plastic, respectively. The effect of lightweighting was likely less significant for J1 because it only rotates the manipulator in the yaw direction and does not work against gravity.

Second, for Joint 2, the peak power consumption was 170 W for A5052, 96 W for Feltcarbon, and 81 W for the 3D-printed version. These results show substantial power reductions of 43.6% and 52.5%, respectively. This significant effect is because J2 must support the combined mass of Link 2 and Link 3 against gravity, requiring much higher torque than other joints. Therefore, lightweighting the structural parts made a major contribution to reducing this joint's power consumption.

Finally, for Joint 3, the peak power consumption was 58 W for A5052, 49 W for Feltcarbon, and 48 W for the 3D-printed version, resulting in modest power reductions of 15% and 18%, respectively. Because J3 only supports the mass of Link 3, which is much lighter than the torque acting on J2, the benefit of lightweighting was not as pronounced.

For the manipulator as a whole (the sum of power consumption of J1, J2, and J3), total power consumption was reduced by 25% for the Feltcarbon version and 30% for the 3D-printed version compared to the A5052 baseline. For comparison, Table IV shows that the total manipulator mass was reduced by 24% for Feltcarbon and 36% for the 3D-printed version. Therefore, the measured reduction in power consumption is largely consistent with the reduction in overall mass. However, a directly proportional relationship was not observed between the mass reduction rate and the power consumption reduction rate, indicating the need to evaluate the impact of factors other than mass reduction, such as operating speed, different trajectories, and manipulator control methods.

It is important to note that these power savings are highly dependent on the task. A greater effect could be expected in applications where the manipulator holds a posture against gravity for extended periods. Conversely, in a fully vertical posture, gravity would have a minimal effect on joint torques. For this reason, these specific results cannot be generalized to all operating conditions. Nevertheless, this study provides a quantitative evaluation of the power savings achieved through lightweighting during a typical pick-and-place operation, demonstrating the effectiveness of this design approach.

IV. Conclusion

We prototyped three versions of a 3-DOF manipulator using different structural materials (aluminum alloy (A5052), Feltcarbon, and 3D-printed plastic (Onyx+CF)) and measured their power consumption during a standardized pick-and-place task. The task, consisting of a 200 mm rise, 500 mm horizontal movement, and 200 mm descent, was repeated for 10 cycles (five full round trips). A comparison of the average power consumption showed that substituting A5052 with Feltcarbon and Onyx+CF reduced the manipulator's total power consumption by 25% and 30%, respectively. The effect was most pronounced at the primary torque acting joint (J2), which exhibited power reductions of approximately 44% (Feltcarbon) and 53% (3D-printed plastic) compared to A5052 manipulator. Conversely, the power-saving effect was less significant for joints closer to the end-effector, where the absolute mass reductions of the supported links were smaller.

In this paper, we evaluated the reduction in power consumption achieved by lightweighting under specific conditions. As future work, a more detailed evaluation should be conducted by assessing factors such as payload capacity, high-speed operation, and movement along other trajectories to clarify the power-saving effects more comprehensively. Furthermore, it is also necessary to examine the influence of the manipulator's control methods on energy consumption. This should include cases where control strategies are introduced, such as those designed to compensate for the creep deformation of the plastic structural parts. Additionally, industrial robots require more than just low power consumption; they also demand high positioning accuracy of the end-effector, operational repeatability, high-speed performance, and high durability. Therefore, for the manipulator investigated in this paper, it is necessary to evaluate several other key performance metrics. These include joint stiffness, absolute and repeatable positioning accuracy, trajectory accuracy, the end-effector's settling time in response to

sudden arm braking, and the effects of long-term operation and environmental influences. Among these metrics, the joint stiffness and the manipulator's response to sudden arm braking are currently under evaluation, and we plan to present these findings in a future publication. Future work will focus on accumulating knowledge of robot arms with plastic structural parts via these evaluations, clarifying design specifications like applicable payload and arm length. We also aim to establish a parts design methodology, including safety factors, for the materials and shapes of these plastic parts. This method should enable the design of appropriate plastic parts based on specifications like payload, size, and external forces. Ultimately, we intend to propose design guidelines for replacing conventional metal components with plastic structural parts.

ACKNOWLEDGMENT

This research is subsidized by New Energy and Industrial Technology Development Organization (NEDO) under a project JPNP20016. This paper is one of the achievements of joint research with ROBOT Industrial Basic Technology Collaborative Innovation Partnership (ROBOCIP).

REFERENCES

[1] M. Brossog, M. Bornschlegl, and J. Franke, "Reducing the energy consumption of industrial robots in manufacturing systems", *The International Journal of Advanced Manufacturing Technology*, Vol.78, No.5, pp.1315-1328, 2015.

[2] F. Stuhlenmiller, J. Jungblut, D. Clever, and S. Rinderknecht, "Combined Analysis of Energy Consumption and Expected Service Life of a Robotic System", *2020 6th International Conference on Mechatronics and Robotics Engineering (ICMRE)*, pp.53-57, 2020.

[3] H. Yin, J. Liu, and F. Yang, "Hybrid Structure Design of Lightweight Robotic Arms Based on Carbon Fiber Reinforced Plastic and Aluminum Alloy", *IEEE Access*, Vol.7, pp.64932-64945, 2019.

[4] X. Wang, D. Zhang, C. Zhao, P. Zhang, Y. Zhang, and Y. Cai, "Optimal design of lightweight serial robots by integrating topology optimization and parametric system optimization", *Mechanism and Machine Theory*, Vol.132, pp.48-65, 2019.

[5] A. Rassõlkin, H. Hõimoja, and R. Teemets, "Energy saving possibilities in the indutrial robot IRB 1600 control", *2011 7th International Conference-Workshop Compatibility and Power Electronics (CPE)*, pp.226-229, 2011.

[6] O. Wigstrom, B. Lennartson, A. Vergnano, and C. Breitholtz, "High-Level Scheduling of Energy Optimal Trajectories", *IEEE Transactions on Automation Science and Engineering*, Vol.10, No.1, pp.57-64, 2013.

[7] T. Otani, M. Nakamura, K. Kimura, and A. Takanashi, "Energy Efficient Path and Trajectory Optimization of Manipulators With Task Deadline Constraints", *IEEE Access*, Vol.11, pp.107441-107450, 2023.

[8] T. Takaki, M. Kanakiyo, and G. Endo, "Damping Characteristics in Adaption of Plastics for Robot Structures", *2023 IEEE/SICE International Symposium on System Integration (SII)*, pp.1-4, 2023.

[9] (Accessed: July 15, 2025) Futaba, "Futaba's CFRP PLATE", https://www.cfrp.mtb.futaba.co.jp/en

[10] Y. Tsukamoto, K. Sekiguchi, H. Nabae, G. Endo, "Measurement of Creep Deformation of Resin Structural Parts for a Lightweight Industrial Robot", *2024 IEEE/SICE International Symposium on System Integration (SII)*, pp.592-597, 2024.

[11] K. Sekiguchi, Y. Tsukamoto, H. Nabae, and G. Endo, "Creep Deformation Measurement of Fiber-reinforced Plastic Materials for Industrial Robot Applications", *2025 IEEE/SICE International Symposium on System Integration (SII)*, pp.320-325, 2025.

[12] (Accessed: July 15, 2025) Markforged, "Onyx", https://markforged.com/materials/plastics/onyx

[13] (Accessed: July 15, 2025) Markforged, "Continuous Carbon Fiber", https://markforged.com/materials/continuous-fibers/continuous-carbon-fiber

[14] (Accessed: July 18, 2025) Kabuku Connect, "A5052", https://www.kabuku.io/guide/metal/aluminum/a5052/

[15] H. Kanazawa, H. Nabae, K. Suzumori, and G. Endo, "Empirical Study for 3D-Printed Robot Design: Dimensional Accuracy of a Hole and Propoal of a New Shaft-Fastening Method", *2022 IEEE/SICE International Symposium on System Integration (SII)*, pp.633-639, 2022.